

BRNO UNIVERSITY OF TECHNOLOGY
Faculty of Electrical Engineering and Communication
Department of Radio Electronics

Ing. Marek Bobula

**CONTRIBUTION TO EFFICIENT USE OF
NARROWBAND RADIO CHANNEL**

Příspěvek k efektivnímu využití úzkopásmového rádiového
kanálu

SHORT VERSION OF PH.D. THESIS

Study field: ELECTRONICS AND COMMUNICATIONS

Supervisor. Doc. Ing. Aleš Prokeš, PhD.

Opponents:

Presentation date:

Keywords

Spectrum efficiency, power efficiency, adjacent channel power, constant envelope modulation, linear modulation, Nyquist filters, rapid frame synchronization, symbol synchronization, software defined digital radio, narrowband land mobile radio, ETSI EN 300 113, dynamic range, FPGA

Klíčová slova

Spektrální účinnost, výkonová účinnost, nežádoucí vyzařování do sousedního kanálu, modulace s konstantní modulační obálkou, lineární modulace, Nyquistova filtrace, rychlá rámcová synchronizace, symbolová synchronizace, softwarově definované rádio, radiostanice pozemní pohyblivé služby, ETSI EN 300 113, dynamický rozsah, FPGA

The manuscript of this thesis is deposited and available:

at the Department of Radio Electronics
Faculty of Electrical Engineering and Communication
Brno University of Technology
Purkyňová 118, 612 00 Brno, Czech Republic

Tel.: +420 541 149 105
Fax: +420 541 149 244
E-mail: urel@feec.vutbr.cz

CONTENTS

1	INTRODUCTION	5
2	LMR TECHNICAL CHARACTERISTICS	6
2.1	LMR receiver parameters	6
2.2	LMR transmitter parameters	7
2.3	Channel fading characteristics	7
3	DIGITAL MODULATION FOR NARROWBAND CHANNEL	8
3.1	Exponential modulations	8
3.2	Linear digital modulation signal models	9
3.3	Digital pulse shaping filter optimization	10
3.3.1	<i>Proposed solution</i>	11
3.3.2	<i>Matched Nyquist filters evaluation</i>	11
4	RAPID FRAME AND SYMBOL SYNCHRONIZATION	12
4.1	Proposed solution	13
4.2	Acquisition, sample wise pattern correlation	14
4.2.1	<i>Adoption the algorithm for the linear modulation techniques</i>	15
4.2.2	<i>Simplified formulation of the algorithm</i>	16
4.3	Tracking, decision directed TED	16
4.3.1	<i>Adoption the algorithm for the linear modulation techniques</i>	17
4.4	Simulation results	18
4.4.1	<i>AWGN channel</i>	18
4.4.2	<i>Rayleigh fading channel</i>	19
5	PROTOTYPE RADIO MODEM ARCHITECTURES	21
5.1	IF over-sampling digital receiver	21
5.2	Measurement results	22
5.3	Efficient use of the radio channel	24
6	CONCLUSION AND FUTURE WORK	25
	REFERENCES	28
	CURRICULUM VITAE	30
	ABSTRACT	31
	ABSTRAKT	32

1 INTRODUCTION

Steadily increasing demand for frequency spectrum, driven in recent years by an overwhelming public interest in wireless communication, has led to an even-greater importance on the spectrum efficiency utilization. From the very advent of the radio transmission, it was evident that a radio device should not only use its occupied channel bandwidth effectively, but, in addition, should also avoid any unnecessary interference with other systems. The frequency spectrum has been proving its importance and has become a scarce resource nowadays. It can be “widened” just by the technical advancements towards its more and more efficient usage.

This dissertation thesis describes one such approach to enhance the spectrum usage of the *land mobile radio* (LMR) system, operating on frequencies between 30 MHz and 1 GHz, with channel separation of up to 25 kHz intended for *private mobile radio* (PMR) networks. This frequency range and especially the VHF band is very well suited for long distance coverage as a primary concern of the LMR communication systems. The PMR systems are mainly used for telemetry, SCADA systems, maritime radio service and are operated by a wide range of users, such as police, companies producing or transporting gas, water, electricity, and in other industrial applications. Although the data traffic generated per user in PMR network is relatively low compared to other wireless systems, there is also a significant need for spectrally efficient modulation techniques which would afford higher network capacity within the same available bandwidth in the future LMR systems.

The narrowband radio devices under consideration are specified mostly by the *European standard ETSI EN 300 113* [1]. Such radio equipments have to face challenging environmental and radio conditions all over the world. The dynamic range in the vicinity of 100 dB, very strict adjacent channel transmitted power attenuation requirements, high data sensitivity, adjacent channel selectivity, high level of radio blocking or desensitization and high co-channel rejection are its most important radio characteristics to mention. It is no wonder that for such high dynamic range demands, super heterodyne receiver structures with a majority of analog components are still widely used. But yet the radio transceiver has to be small in dimensions, consumes low power and remains all its parameters over the wide industrial temperature range and over extensive period of time for reasonable price. At the same time, it should provide enough flexibility to accommodate different channel bandwidths, digital modulation formats, data rates, and techniques, to combat negative effects of the radio channel. From this point of view, the *software defined radio* (SDR) concept is, indisputably, a prospective alternative and has not been widely used by these systems [2], [3]. The rapid expansion of the digital signal processing, together with the advancements in signal analog-to-digital converters technology have, in recent years, made such projects economically manageable.

The today’s LMR systems, being subject to [1], use mostly exponential constant envelope modulations GMSK and 4-CPFSK. The application of the continuous phase modulations is mainly due to the extreme *adjacent channel transmitted power* (ACP) attenuation requirements, and inherent robustness against channel nonlinearities. Relatively simple implementation of the non-coherent demodulators and synchronization algorithms also significantly contributes to the efficient channel usage, especially in packet-based switching networks. The systems thus maintain good power efficiency while the spectral efficiency reaches compromising values not exceeding 1 bit/s/Hz.

The strict limitations of the referenced standard as well as the state of the technology, has hindered the increase in *communication efficiency*, with which the system has used its occupied bandwidth. New modifications and improvements are needed to the standard itself and to the up-to-date architectures of narrowband LMR devices, to make the utilization of more efficient modes of system operation practically realizable. The main objective of this dissertation thesis is therefore to find a practical way how to combine the favorable properties of the advanced nonlinear and linear digital modulation techniques in a single digital modem solution, in order to

increase the efficiency of the narrowband radio channel usage allocated to the new generation of the industrial LMR devices. The thesis presented contributes to this general objective in following areas:

- Analysis and application of the enhanced digital modulation formats for the next generation of narrowband land mobile radio system in order to improve its spectral efficiency, while respecting its specific characteristics in form of high power efficiency, robustness against interference and fast signal acquisition needed for rapid packet switching.
- In order to effectively fulfil very strict limits of adjacent channel power, new class of Nyquist filters called Nyquist δ -filters has been formulated and analyzed in detail.
- The analysis of the exponential modulations creates a significant part of this thesis as these techniques are still the major modulation formats used by the LMR radios. There is a closer description of the digital algorithms for frequency discrimination as a core algorithm of the software defined modem. Two refinements to the techniques available in technical literature are presented which can improve the signal-to-noise ratio of the demodulated signal [4].
- The problem of rapid frame and symbol synchronization applicable for exponential and linear mode of narrowband LMR system operation creates a significant part of the thesis. The algorithm formulation and analysis is covered in Chapter 4, and towards the end of 2010, it has been implemented successfully in a new generation of radio modems utilizing 2-CPFSK, 4-CPFSK and $\pi/4$ -DQPSK modulations.
- Design and analysis of the two prototyping architectures for IF (*intermediate frequency*) sampling software defined narrowband radio modems. Giving the complete measurement results of the essential radio parameters of the two possible architectures, this part of the work identifies the main factors influencing the instantaneous dynamic range performance, and gives several practical design recommendations in order to increase the efficiency of the narrowband radio channel utilization.

2 LMR TECHNICAL CHARACTERISTICS

To understand the motivation behind the main objective, it is, first, necessary to briefly describe the essential technical parameters – particularly their limits – required upon the LMR system. First of all, the characteristics of the radio receiver and transmitter are given, followed by the main characteristics of the narrowband communication channel as a physical medium through which the signal passes from the transmitter to the receiver.

2.1 LMR RECEIVER PARAMETERS

The most important parameters which have a strong influence on how the narrowband LMR is designed are a *maximum usable (data) sensitivity*, *co-channel rejection*, *adjacent channel selectivity* and *blocking or desensitization*. In this work their definitions and requested limits are a subject to European standard ETSI EN 300 113 [1]. It is important to note that all the following radio parameters and limits are requested for conformity testing only, to ascertain if the radio device under consideration is capable of *listen-before-talk* (LBT) mode. While it is the case of the intended narrowband radio system, the radio parameters are considered essential in this work. Where needed, the test signals and all other details, such as measurement procedures, are also assumed to be the subject of referenced standard, unless otherwise noted.

- The *maximum usable sensitivity* shall not exceed an electromotive force of **3.0 dB μ V** under normal test conditions.

- The value of the *co-channel rejection* ratio shall be between **-8.0 dB** and **0 dB**, for channel separations of **25 kHz**.
- The value of the *adjacent channel selectivity* for channel separation of **25 kHz** shall not be less than **70 dB**.
- The *blocking* ratio for any frequency within the specified ranges shall not be less than **84 dB**, except at frequencies on which spurious responses are found.

Communication system with specified limits of maximum data sensitivity and co-channel rejection can be according to [5] classified as *power-limited*. With the assumption that today's LMR systems already use the most spectrally efficient modulation, the only way to increase the data rate – in a given coverage area – seems to be to widen the system bandwidth together with the transmitted signal power. As is shown in the next paragraph, due to the strict transmitter characteristics, this primary assumption cannot be the case for the narrowband LMR system.

2.2 LMR TRANSMITTER PARAMETERS

In this section, two essential radio transmitter parameters are identified to have a crucial influence on an overall system performance. Those are *the adjacent channel power* (ACP) and *the transmitter power efficiency*. The first has a direct impact on the spectrum efficiency of the LMR system and the latter is considered an important issue in order to minimize the overall system power consumption.

- For a channel separation of 25 kHz, the ACP shall not exceed a value of **60 dB** below the transmitter power without the need to be below 0.2 μW (-37 dBm).
- The practical way of evaluating the transmitter efficiency is to find the ratio of the transmitted output power and the overall input power level of the transmitting system, while the transmitter is operating under defined conditions of modulation and the ACP requirements are satisfied.

It is important to note that, until 07/2007, the standard strictly demanded the adjacent channel power ratio of -70 dB. The ACP parameter is particularly important in LMR systems, since it influences the density of the channels that can be used in a given area. Its value originated in the use of the traditional analog *frequency modulated* (FM) radio systems. Ironically, it was one of the main limitations for why those systems were – for many years – not able to utilize spectrally more efficient modulation schemes [6].

As it was written in Section 2.1, the LMR under consideration can be classified as a power limited system. By a closer examination of the demanding limits of ACP it has to be regarded also as *strictly bandwidth limited*. For such systems, the only way to increase the data rate is to use more bandwidth-efficient modulation schemes [5]. One can now either take back the early assumption that today's LMR system already utilizes the most spectrally efficient modulation techniques possible and try to find more suitable signaling techniques (meaning modulation and coding), or one can compromise the data rate over the decreasing signal level. With the partial lessening in ACP parameter requirement to -60 dB, both of the assumptions should be practically applicable.

2.3 CHANNEL FADING CHARACTERISTICS

Respecting the small scale multipath fading categorization published in [7], the radio channel under consideration is assumed as time-variant, experiencing *slow frequency flat fading* mechanism. When viewed in the time domain, the radio channel is said to be frequency flat if all of the significant received multipath components of a symbol arrive within the symbol time duration T . And, the channel is referred to as introducing slow fading if the channel state remains virtually unchanged during the time of the modulation symbol.

For practical radio channel simulation, in this work, the simplified radio channel models *typical urban* (TU50) and *highly terrain* (HT200) at reference frequency of 400 MHz – defined in [8] – have been used. The models exhibit a few discrete paths which are mutually statistically independently fading. The signal tap (component) in each path is assigned its relative delay and its average relative power of the complex tap-gain process. The fading process in each path is assumed to be stationary Gaussian process with a power density function equal to the classical Doppler spectrum (2.1) normalized by the maximum Doppler shift

$$S(f) = \begin{cases} \frac{1}{\pi f_d \sqrt{1 - \left(\frac{f}{f_d}\right)^2}} & \text{for } -f_d \leq f < f_d \\ 0 & \text{elsewhere} \end{cases}, \quad (2.1)$$

where f_d is the maximum Doppler shift frequency, defined as the ratio of the relative transmitter-receiver velocity and the wavelength calculated at a nominal frequency (400 MHz)

$$f_d = \Delta v / \lambda_0. \quad (2.2)$$

All the particular parameters of the channel models can be found in [4].

3 DIGITAL MODULATION FOR NARROWBAND CHANNEL

The use of exponential digital modulations and particularly the *continuous phase modulation* (CPM) in narrowband LMR was motivated mainly due to the extreme ACP attenuation requirements and inherent robustness against the channel nonlinearities. Relatively simple implementation of the non-coherent demodulators and synchronization algorithms also significantly contributed to the efficient channel usage, especially in packet based switching networks. The M-CPFSK in this case is recognized as a general class of the non-linear or exponential digital modulation.

3.1 EXPONENTIAL MODULATIONS

Following the typical signal notations [9] the information – modulation – signal to be transmitted can be written as

$$m(t, \alpha_k) = \sum_{k=-\infty}^{\infty} \alpha_k h(t - kT), \quad (3.1)$$

where α_k are the data symbols taking on the values from the real symbol alphabet $\pm 1, \pm 3, \dots, \pm M-1$, T is the symbol period and $h(t)$ is the frequency pulse or an impulse response of the pulse shaping filter. Obviously, the modulation signal $m(t, \alpha_k)$ is a superposition of the modulation impulses weighted by the information symbols. Due to the requirement for continuous phase change, the relation between the frequency pulse $h(t)$ and phase pulse $q(t)$ in all CPM modulations is defined as

$$q(t) = \int_{-\infty}^t h(\tau) d\tau, \quad (3.2)$$

thus the resulting continuous phase $\psi(t, \alpha_k)$ of the modulated signal changes in time according to

$$\psi(t, \alpha_k) = 2\pi h \sum_{k=-\infty}^{\infty} \alpha_k q(t - kT), \quad (3.3)$$

where h is the *modulation index* describing the relation between the *maximum frequency deviation* Δf and the *symbol rate* R according to

$$h = \frac{2\Delta f}{R(M-1)}. \quad (3.4)$$

It also defines how much the phase changes during the symbol period respecting the symbol value of α_k . The resulting complex envelope $s(t)$ of the M-CPFSK modulated signal can be then written as

$$s(t) = \exp \left\{ j 2 \pi h \left[\sum_{k=-\infty}^{\infty} \alpha_k q(t - kT) \right] \right\}, \quad (3.5)$$

which can be further modified into (3.6) corresponding to the conventional analog FM signal

$$s(t) = \exp \left\{ j 2 \pi k_{FM} \int_{-\infty}^t \left[\sum_{k=-\infty}^{\infty} \alpha_k h(\tau - kT) \right] d\tau \right\}, \quad (3.6)$$

where k_{FM} is a frequency modulator sensitivity per modulation state defined as

$$k_{FM} = \frac{\Delta f}{(M-1)}. \quad (3.7)$$

The symbol alphabet assumed in this work is uniformly distributed and the modulation index is a constant for selected modulation setting.

3.2 LINEAR DIGITAL MODULATION SIGNAL MODELS

Similarly to the modulation signal used for exponential modulation, the complex modulation envelope of the linearly modulated signal can be written as a linear superposition of the modulation impulses weighted by the information symbols

$$s(t) = m(t, \alpha_k) = \sum_{k=-\infty}^{\infty} \alpha_k h(t - kT) = s_I(t) + js_Q(t). \quad (3.8)$$

In case of linear modulation, α_k is the train of the *complex* modulation symbols as oppose to the *real* symbols in (3.1). The complex modulation symbols α_k are usually plotted in complex plane, regardless of the time scale, and form a *constellation* of the digital modulation. For a given modulation pulse shape $h(t)$ that defines the spectrum of the modulated signal, it is just the modulation constellation and the allowed transitions between the constellation points that distinguishes between various modulation formats. Thus, innumerable modulation formats exist. However from the prospective of the narrowband radio design, the constant envelope constellations are of the utmost importance, since they minimize the amplitude variations of the modulated signal. It can be shown [5], that the lower the modulation envelope variations, the lower the amount of the spectral re-growth and self interference due to the channel nonlinearities. As the evaluation criterion the PAPR of the modulation envelope (3.8) of the given modulation scheme can be calculated as

$$PAPR = \frac{\max \left\{ |m(t, \alpha_k)|^2 \right\}}{E \left\{ |m(t, \alpha_k)|^2 \right\}}, \quad (3.9)$$

where E assigns the expectation function over the sufficiently long signal interval.

If the modulation symbols α_k result from a differential encoding, the digital modulation format is called differential. The differential encoding and decoding is known [10] to be very robust against

fast signal fading effects and has the advantage of non-coherent detection at the receiver. On the other hand, at the same SNR ratio the differential encoded modulation format typically experiences higher BER than its non-differentially encoded counterpart. The combination of both properties – minimum modulation envelope amplitude variations and differential encoding – yields to the widely used single carrier modulation techniques named $\pi/4$ -DQPSK, $\pi/8$ -D8PSK. In order to further improve the bandwidth efficiency, the 16-QAM modulation, with a star constellation diagram [10], can be used. It has an advantage in that the star ordering of the constellation points can carry a differentially encoded modulation signal. Such a modulation format is therefore referred to as *16-state differentially encoded quadrature amplitude modulation* (16-DEQAM). In Table 3.1, there is a comparison of the theoretical spectrum efficiencies and PAPR values for two levels of excess bandwidth parameter.

Based on the modulation properties simulations [4], the $\pi/4$ -DQPSK, D8PSK and star 16-DEQAM can be recommended for future implementation into narrowband LMR system. More detailed description of the intended modulation formats can be found in the full text thesis [4].

Table 3.1: Comparison of the linear digital modulation techniques. The PAPR parameter (3.9) is stated for two excess bandwidths [4].

Modulation	η	PAPR ($\alpha=0.25$)	PAPR ($\alpha=0.35$)	non-coherent
[-]	[bit/s/Hz]	[dB]	[dB]	[-]
QPSK	2	5	3.7	no
OQPSK	2	4	3	no
DQPSK	2	5	3.7	yes
$\pi/4$ -DQPSK	2	4.3	3.2	yes
$\pi/4$ -FQPSK	2	3.7	2.7	yes
8DPSK	3	4.5	3.5	yes
$\pi/8$ -8DPSK	3	4.5	3.5	yes
16-QAM	4	6.5	5.5	no
16-DEQAM	4	5.5	5	yes

3.3 DIGITAL PULSE SHAPING FILTER OPTIMIZATION

The spectrum of the exponentially modulated signal cannot be considered strictly band limited, similarly to the most linear digital modulation formats. However, the shape of the phase or frequency pulse significantly influences [11] the spectrum of the transmitted signal (3.5). A truncated version of the *square root raised cosine* (RRC) pulse shaping filter as a typical representation of the Nyquist filter for the excess bandwidth greater than zero is usually implemented in LMR systems when using 4-CPFSK modulation. Such filters have limited stop-band attenuation and thus the system designers are forced to use very low roll-off factors approaching the value of 0.2 and therefore higher group delays of more than 8 symbols [12].

The demand for the matched pulse shaping filters with high stop-band attenuations is even more severe in case of the linear modulation techniques. It can be shown [4], that the typical truncated version of the RRC filters can reach the ACI levels of -60 dBc required, with very high group delays and therefore very high orders of the digital filters.

In the following section, a new set of Nyquist filters is briefly described. Compared to already existing Nyquist filter sets, the proposed filters strike a balance between time- and frequency-domain parameters in favor of filter stop-band attenuation, while reaching low residual ISI. By a number of filter examples, this part of the work [4], [13] shows that the proposed Nyquist δ -filter can be a preferable option for the application in LMR systems that need to fulfill strict limits of adjacent and alternate channel power attenuation.

3.3.1 Proposed solution

A closer analysis of the equation describing the frequency characteristic of RC filter unveils the fact that it is a convolution of a rectangular pulse of duration $1/2T$ and a RC window modified by the roll-off parameter. As shown in [14], there are other window shapes that can converge to zero more smoothly. A good alternative is a generally defined *Blackmann window*, which can be continuously changed to the *Blackmann*, *exact-Blackmann*, *Blackmann-Harris* and $\cos^4(x)$ windows by changing the values of a_0 , a_1 and a_2 in its definition

$$w(x) = a_0 + a_1 \cos(\pi x) + a_2 \cos(2\pi x) \quad (3.10)$$

Although the general Blackmann window smoothly converges to zero level, it does so at the expense of the window width, and its shape does not satisfy the vestigial symmetry property. Nevertheless, there is still the possibility of decomposing the window into its upper and lower parts and using these functions to construct a Nyquist filter by shifting them to the right by a distance marked δ . Respecting the typical notation of the Nyquist RC filters, a general *Nyquist δ -filter* defined in the frequency domain can thus be written as [13]

$$G_\delta(f) = \begin{cases} 1, & 0 \leq f \leq B(1-\alpha) \\ 1 - a_0 - a_1 \cdot \cos \frac{\pi[B(1+\alpha_0) - (f + \delta)]}{2B\alpha_0} - a_2 \cdot \cos 2 \frac{\pi[B(1+\alpha_0) - (f + \delta)]}{2B\alpha_0}, & B(1-\alpha) < f \leq B \\ a_0 + a_1 \cdot \cos \frac{\pi[B(1+\alpha_0) - (f - \delta)]}{2B\alpha_0} + a_2 \cdot \cos 2 \frac{\pi[B(1+\alpha_0) - (f - \delta)]}{2B\alpha_0}, & B < f \leq B(1+\alpha) \\ 0, & B(1+\alpha) \leq f \end{cases}, \quad (3.11)$$

where

$$\delta = 0.5 - B(1 - \alpha_0) - \frac{2B\alpha_0}{\pi} \left[\pi - \arccos \left(\frac{1}{4} \frac{a_1 - \sqrt{a_1^2 + 8a_2^2 + 4a_2 - 8a_2a_0}}{a_2} \right) \right]. \quad (3.12)$$

In (3.12), B is the single-sided filter bandwidth corresponding to $1/2T$, and α is the *excess bandwidth* parameter usually called *roll-off factor*. It is important to note that the Nyquist δ -filter differs from the RC filter also in the starting point of its stop-band region and its first null bandwidth. Therefore, to get the filter definition directly comparable to that of the RC filter, its notation is adopted where

$$\alpha_{RC} = \alpha = \alpha_0 + \delta. \quad (3.13)$$

3.3.2 Matched Nyquist filters evaluation

There are three important characteristics to evaluate matched Nyquist filters of the same order and filter class (FIR, IIR). From the time-domain parameters it is the residual ISI level and the decay of the cascaded impulse response side lobes level. In frequency-domain, it is the stop-band attenuation of the square root filter variant. The detailed numerical comparison of the studied

Nyquist filters can be found in [4], [13]. At this place a single example has been chosen to demonstrate the properties of the proposed Nyquist δ -filter (3.12), (3.13). In Figure 3.1, there are amplitude frequency characteristics of the square root Nyquist filter variants (root raised cosine – RRC; root Nyquist filter designed according to [15] – RBN; proposed root Nyquist δ -filter – RND) clearly unveiling the significant differences in stop-band attenuation. From the eye diagrams shown in Figure 3.2, the two facts are evident. Firstly, the residual ISI level is lower for the Nyquist δ -filter, but on the other hand the side lobes level of the Nyquist δ -filter filter is higher which can be noticed by comparing the maximum signal swings. This results in narrower eye opening, the price we have to pay for better stop band attenuation in frequency-domain.

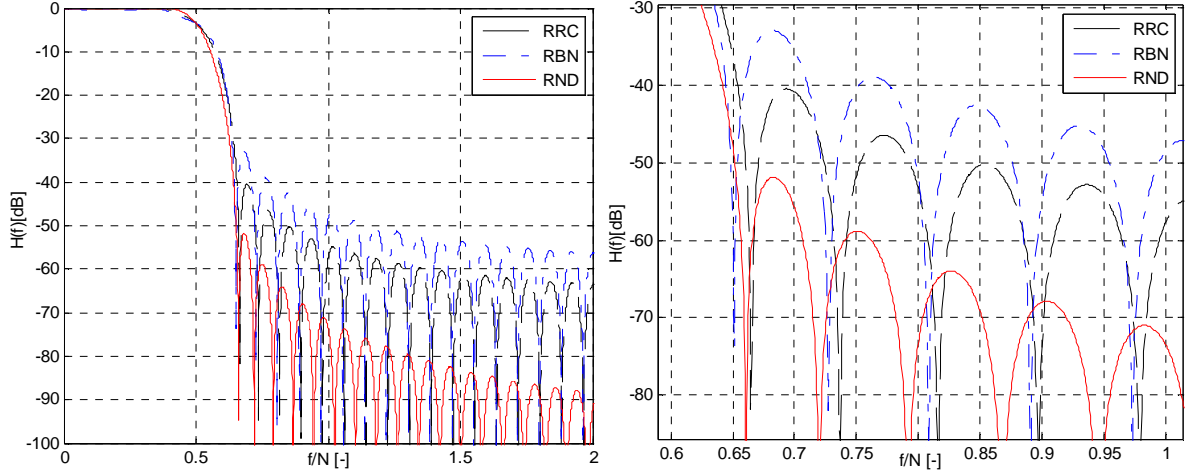


Figure 3.1: Amplitude frequency characteristics (log scale) of the truncated square root RC filter (RRC); square root B-filter (RBN); square root Nyquist δ -filter (RND) of the same parameters: $\alpha=0.284$ (excess bandwidth); $G_D=6$ (filter group delay); $N=5$ (over-sampling ratio); $N_O=60$ (digital filter order).

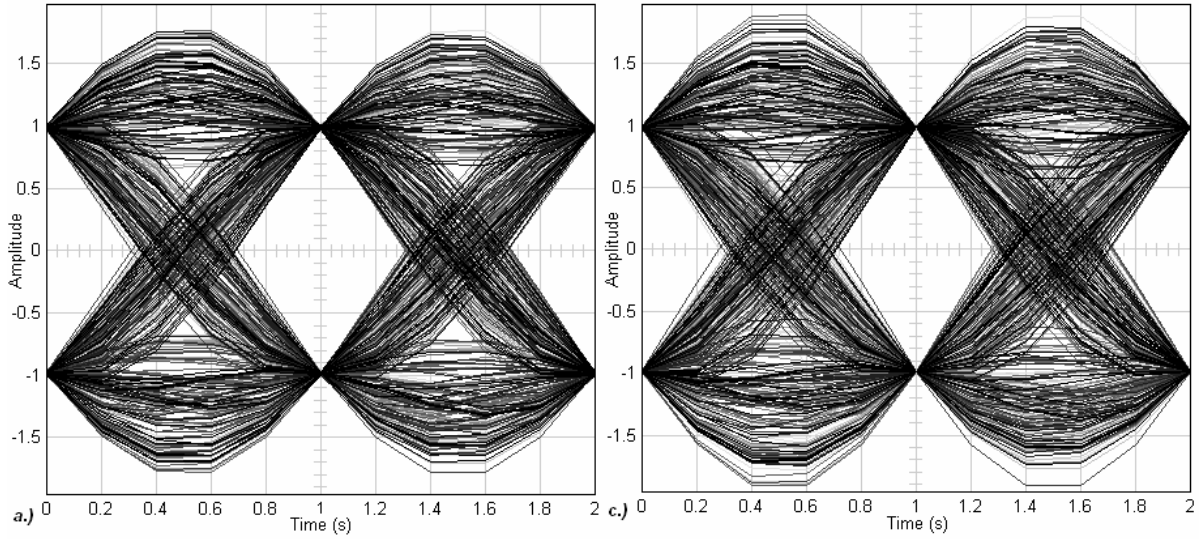


Figure 3.2: Eye diagrams of the transmitter and receiver cascade a.) RC filter; c.) Nyquist δ -filter, $\alpha=0.284$; $G_D=12$; $N=5$; $N_O=120$.

4 RAPID FRAME AND SYMBOL SYNCHRONIZATION

The communication system – for which the narrowband LMR equipment is intended – exclusively uses a packet or frame based multiple channel access. It is, either stochastic multiple channel access technique, or *carrier sense multiple (channel) access* (CSMA) with collision detect and

acknowledgements. In this case, the radio receiver's only priory information about the opposite transmitter(s) is the information about the nominal frequency and the symbol rate selected. There are various frame lengths used, ranging from a couple of bytes e.g. 12, up to the maximum of 1500 bytes. The typical receive to transmit attack time is around 1.5 ms.

Such requirements place very strict demands on the synchronization algorithms, which have to extract all the possible information about frequency, frame and symbol synchronization within the first symbols of the incoming frame. It is obvious that, the shorter the acquisition time the higher the communication efficiency of the LMR system can be achieved. However, in case the system does not, or cannot, have all the realizations of the random process, the only way of estimating its parameters is to make use of the time demanding ensemble average of the required parameter [16]. This basically means that the higher the accuracy of the estimated parameter that is required, the longer the averaging periods are needed. This is a major reason that complicates the use of the non-data aided synchronizers in radio data packet switching systems. Methods based on an a priori known preamble symbols are preferred since the preamble represents a single realization of the random process of known parameters, however corrupted by the radio channel. With today's digital signal processing capability these tasks can be enhanced further by developing more and more sophisticated algorithms, but care must be taken when trading off the performance gained by such algorithms and their complexity.

It is the aim of the present chapter to propose and analyze a complete frame and symbol timing recovery concept suited for narrowband burst mode communication system utilizing modulation techniques chosen in Chapter 3, and to analyze in details its main building blocks needed for acquisition and tracking phase. For LMR systems, where the computational power is always very limited and the frame and symbol timing synchronization is to be combined in rapid synchronization algorithm, *the sample wise pattern correlation technique* with a combination of *the decision directed adaptive synchronization algorithm* is proposed. The concept can be simply modified for all digital modulation techniques chosen, and yields satisfactory results, as it is shown by the overall system simulation under AWGN and fading channel conditions.

4.1 PROPOSED SOLUTION

Following the signal models derived in Section 3, the received signal at the input to the synchronization algorithm can be described as

$$y[i] = A(kT + nT_s - \tau_0) \exp[j\psi(kT + nT_s - \tau_0; \alpha_k)] \exp[j2\pi\nu(kT + nT_s) + \theta] + v[i] \\ -\infty \leq i \leq \infty; \quad -\infty \leq k \leq \infty; \quad 0 \leq n \leq (N-1) \quad (4.1)$$

In (4.1), k is the modulation symbol index, i is the general sample index and n is the digital sample index within the specific interval. N is the over-sampling ratio describing the number of samples within one modulation symbol. The parameters assigned as ν , θ and τ are the unknown values of frequency offset, initial carrier phase and symbol timing epoch respectively. The $v[i]$ assigns a single realization of the band-limited noise process. It is a purpose of the synchronization algorithms to extract and compensates for initial timing offset τ_0 and to follow its characteristic in time as precisely as the single realization of the random process forming the receiving frame permits.

The simplified block diagram of the proposed symbol and frame timing recovery scheme is shown in Figure 4.1. The input to the algorithm is the baseband representation of modulated signal $y[i]$. For the case that the signal is modulated by the nonlinear modulation technique, the *frequency discrimination* block [4], together with the *matched filtering* is needed prior to the synchronization process itself. If the linearly modulated signal is entering the *differential demodulator*, it is assumed that the signal has already been filtered by the receiver matched filter (Chapter 3). The common feedback algorithm of the symbol timing recovery comprising the timing adjustment

block (*Fractional Interpolator*) [4],[17], timing error detector (*Symbol Timing Error Detector*) and loop filter is proposed to be supplemented by the sample wise pattern correlation [18] block (*Frame Synchronization, Symbol Timing Acquisition*) to acquire frame synchronization and to provide the initial timing estimate for the feedback algorithm. In the following sections, the brief description of the sample wise pattern correlation algorithm and the symbol timing error detector is given. In [4], [17], [18] the closer description and analysis can be found. At this place, the main intention is to introduce the proposed concept and present the algorithms' modifications. In addition, it is to demonstrate that the algorithm can be simply modified for all digital modulation techniques chosen, and yields satisfactory results, as shown by the overall system simulation under AWGN and fading channel conditions.

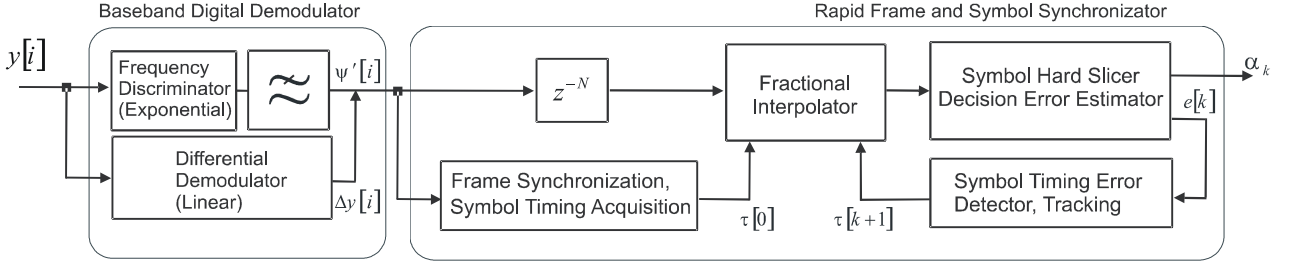


Figure 4.1: Simplified block diagram of the rapid frame and symbol synchronization concept with its main part.

4.2 ACQUISITION, SAMPLE WISE PATTERN CORRELATION

Let suppose that the distortion less frequency discrimination is already employed in the system as well as the matched filtering by a square root Nyquist filter of any of the characteristics studied in Section 3.3. The incoming signal can be written in a simplified general notation as

$$y[i] = \begin{cases} A(i - \tau_0)x(i - \tau_0) + v[i] & 0 \leq i \leq (L_0N - 1) \\ v[i] & \text{otherwise} \end{cases}, \quad (4.2)$$

where $x(i - \tau_0)$ can be seen as the original preamble signal with the symbol length of L_0 , which optimal sampling instant τ_0 is to be estimated. The $v[i]$ represents the realization of noise process which is statistically independent from the preamble signal $x(i - \tau_0)$. N is the over-sampling factor. $A(i)$ is the general time variant amplitude of the incoming signal.

As shown in [4], for the applications with limited amount of signal processing resources, the reduction of the signal resolution in amplitude rather than in time by reducing the over-sampling factor can be a suggested option. In the utmost situations only the information about the signal polarity can be used to calculate the correlation function with a priori bipolar preamble pattern assign as $h[k] = x[L_0 - k - 1]$

$$R_{xy}(\tau) \approx R_{xy}[i] = \sum_{k=0}^{L_0-1} \text{sign}(y[i - kN]) \text{sign}(h[k]) \quad -\infty \leq i \leq \infty, \quad (4.3)$$

where $\text{sign}(\cdot)$ denotes the bipolar signum function

$$\text{sign}(x) = \begin{cases} 1 & x \geq 0 \\ -1 & \text{otherwise} \end{cases} \quad (4.4)$$

The signum function can be seen as an application of a limiter to the incoming signal which normalizes the information about the signal amplitude and thus solves the problem of the cross-correlation maximum dependency on time variant signal amplitude.

The central point of the cross-correlation function maximum is in direct relation to the maximum eye opening of the demodulated signal and represents the optimal sampling point. Thus, it can be used not only for the frame synchronization but also for symbol timing estimation.

Even though the (4.3) represents already a straightforward approach, it can be simplified even further. In (4.3), the bipolar signalling can be changed into unipolar and the multiplication into an XOR operation denoted as \oplus

$$R_{xy}(\tau) \approx R_{xy}[i] = \sum_{k=0}^{L_0-1} \text{sign}(y[i - kN]) \oplus \text{sign}(h[k]) \quad -\infty \leq i \leq \infty, \quad (4.5)$$

where, in this case, the $\text{sign}(x)$ denotes the unipolar signum function defined by

$$\text{sign}(x) = \begin{cases} 1 & x \geq 0 \\ 0 & \text{otherwise} \end{cases}. \quad (4.6)$$

The required information about the frame and symbol synchronization is now carried in a minimum of the correlation function $R_{xy}[i]$. The main advantages of this modification are that the algorithm is no more dependent on the preamble length L_0 , the threshold detection is greatly simplified and the computational requirements are substantially reduced.

4.2.1 Adoption the algorithm for the linear modulation techniques

Direct adoption of the proposed synchronization mechanism to the linear modulation techniques (Section 3.2) is complicated mainly by the fact that the maximum of the cross-correlation function is strictly dependent on the receiving signal frequency offset [4], which is always present at the beginning of the received frame. While this phenomenon is a minor issue for exponentially modulated signal processing, it requires a special attention when implementing the synchronization task for linearly modulated signal. For the LMR communication system utilizing the selected linear modulation techniques, the problem described can be effectively overcome by the differential encoding and decoding of the preamble sequence in the same manner as the data sequence is encoded.

Let us assume the receive signal has already been down converted to baseband and filtered by a square root Nyquist filter of any of the characteristics studied in Section 3.3. Similarly to (4.2) the receive signal can be written as

$$y[i] = \begin{cases} A(i - \tau_0)x(i - \tau_0)\exp(j2\pi\Delta f T_s(i - \tau_0)) + v[i] & 0 \leq i \leq (L_0N - 1) \\ v[i] & \text{otherwise} \end{cases}, \quad (4.7)$$

where in case of linear modulation, the $x(i - \tau_0)$ is representing the original *complex* baseband preamble signal with the symbol length of L_0 , which optimum sampling instant τ_0 is to be estimated. The Δf represents the overall frequency offset between the transmitting and receiving radio modem. The $v[i]$ represents the realization of noise process which is statistically independent from the preamble signal $x(i - \tau_0)$. N is the over-sampling factor. Now the cross-correlation with the differentially encoded preamble pattern can be calculated as

$$R_{xy}[i] = \sum_{n=0}^{L_0N-1} \Delta y[i - n] \Delta x^*[L_0N - n - 1], \quad (4.8)$$

$$R_{xy}[i] = \exp(j2\pi\Delta f T_s N) \sum_{n=0}^{L_0N-1} \Delta x[i - n] x^*[L_0N - n - 1] + \sum_{n=0}^{L_0N-1} \Delta v[i] x^*[L_0N - n - 1]. \quad (4.9)$$

From (4.9) it can be realized that, if the second term in (4.9) is omitted, the cross-correlation maximum is degraded only by a single and constant phasor $\exp(j2\pi\Delta T_s N)$. Moreover, the symbol period can be recognized where

$$T = NT_s, \quad (4.10)$$

and, therefore it can be concluded that the degradation of the cross-correlation maximum due to the frequency offset is independent also of the over-sampling factor. This, however, is a preferable property which enables to use either higher number of samples per modulation symbol or use an over-sampling to locate the optimum sampling point more precisely without the degradation of correlation maximum due to the frequency offset.

4.2.2 Simplified formulation of the algorithm

The hardware realization of the complex differential demodulator is straightforward and follows exactly the definition [4]. When it comes to complex correlator the direct implementation of (4.8) yields to demanding processing structures containing four FIR filters with their output summed together. Besides the complexity, also the previously described problems with cross-correlation maximum variation over the signal level, as well as the correct threshold detection have to be taken into account when (4.8) is used for symbol synchronization.

Following the same reasoning as in previous section the (4.8) can be rewritten into

$$R_{xy}(\tau) \approx R_{xy}[i] = \sum_{k=0}^{L_0-1} \text{sign}(\Delta y[i - kN]) \oplus \text{sign}(\Delta x^*[L_0 - k - 1]), \quad -\infty \leq i \leq \infty, \quad (4.11)$$

where the $\text{sign}(x)$ function is defined as

$$\text{sign}(x) = \begin{cases} [0 \ 0] & \Re(x) \geq 0; \Im(x) \geq 0 \\ [0 \ 1] & \Re(x) < 0; \Im(x) \geq 0 \\ [1 \ 1] & \Re(x) < 0; \Im(x) < 0 \\ [1 \ 0] & \Re(x) \geq 0; \Im(x) < 0 \end{cases}. \quad (4.12)$$

This modification simplifies the overall complex correlation structure and unifies the acquisition mode of the symbol and frame synchronization task for all the selected linear modulation formats.

4.3 TRACKING, DECISION DIRECTED TED

In this section, the main attention is focused on the second approach to be used in symbol timing synchronization process while analyzing the adaptive algorithm for the symbol timing error detection based on non-data aided symbol decisions.

The description of the algorithm can be started from the base concept of the minimization of mean-squared error MSE of the detected signal [51], [54] where the objective function is defined as

$$\mathcal{E}_k^2 = E\{e[k]^2\} \rightarrow \min, \quad \forall k, \quad (4.13)$$

here k is the symbol index. Ideally, the error signal can be calculated as

$$e[k] = x[k] - y[kT + \tau]. \quad (4.14)$$

In this equation, the $x[k]$ is the transmitted data symbol which is either real value signal for the case of exponential modulation or complex signal in case of linear modulation. In the following,

the real signal alternative is assumed for the description simplicity. The same assumption is made for the received signal $y[k]$.

Since the receiver does not have the information about the transmitted symbols, the signal $x[k]$ is replaced by its local estimate $\hat{x}[k]$ or the decisions yielding $\hat{x}[k]$. If the initial timing phase τ_0 has been successfully acquired by the previous block (Section 4.2), it is very likely that both symbol sequences are the same, thus

$$x[k] = \hat{x}[k]. \quad (4.15)$$

It can be shown [4] that application of this principle yields a recursive adaptation algorithm to minimize the MSE of the detected signal while updating the timing phase towards its optimum value according

$$\tau[k+1] = \tau[k] + 2\mu \left\{ e[k] \frac{\partial y[kT + \tau]}{\partial \tau} \right\}. \quad (4.16)$$

In (4.16) the μ is the step-size parameter influencing the rate of convergence and algorithm stability.

The derivation of the received signal in (4.16) can be approximated by a discrete time differentiation over the selected time interval and its angular coefficient describes the direction towards the optimum sampling instant. Using this approximation the term for derivation can be rewritten as

$$\frac{\partial y[kT + \tau]}{\partial \tau} \approx \frac{y(kT + \tau + \Delta\tau) - y(kT + \tau - \Delta\tau)}{2\Delta\tau}. \quad (4.17)$$

In the case of where the differentiation interval is equal to one half of the sampling period T_s , (4.17) reduces further and if substituted into (4.16) yields to equation suitable for the digital implementation

$$\tau[k+1] = \tau[k] + \frac{2\mu}{T_s} e[k] \{ y[kT + \tau] - y[kT + \tau - T_s] \} \quad 0 \leq k < \infty. \quad (4.18)$$

4.3.1 Adoption the algorithm for the linear modulation techniques

The efficient method to process the signal modulated by the differential linear modulations is by processing the phase of the incoming signal followed by calculating the phase difference and assigning a respective symbol that has most likely been transmitted.

For the case of $\pi/4$ -DQPSK the tasks needed to be calculated are as follows. The calculation of the signal phase (4.19) followed by its differential decoding (4.20) and (4.21)

$$\psi[i] = \arctg \left\{ \frac{\Im(y[i])}{\Re(y[i])} \right\}, \quad (4.19)$$

$$\Delta\psi[i] = \psi[i] - \psi[i - N], \quad (4.20)$$

$$\alpha_k = \begin{cases} [0 \ 0] & \Delta\psi_k \geq 0; \Delta\psi_k < \frac{\pi}{2} \\ [0 \ 1] & \Delta\psi_k \geq \frac{\pi}{2}; \Delta\psi_k < \pi \\ [1 \ 1] & \Delta\psi_k \geq \pi; \Delta\psi_k < \frac{3\pi}{2} \\ [1 \ 0] & \Delta\psi_k \geq \frac{3\pi}{2}; \Delta\psi_k < 2\pi \end{cases}, \quad (4.21)$$

where $\varphi[i]$ can be seen as an estimate of the instantaneous signal phase $\psi[i]$.

The formulation of the decision directed symbol timing recovery algorithm can be thus, written as

$$\tau(k+1) = \tau(k) + 2\mu \left\{ e[k] \frac{\partial \Delta\psi[kT + \tau]}{\partial \tau} \right\} \quad 0 \leq k < \infty, \quad (4.22)$$

where $e[k]$ is the real error signal defined as

$$e[k] = \Delta\psi[k] - \Delta\psi[kT + \tau], \quad (4.23)$$

as well as the result of the phase change differentiation

$$\frac{\partial \Delta\psi[kT + \tau]}{\partial \tau} \approx \frac{\Delta\psi[kT + \tau] - \Delta\psi[kT + \tau - T_s]}{T_s}. \quad (4.24)$$

4.4 SIMULATION RESULTS

The scope of this chapter is to evaluate the overall performance of the proposed frame and symbol synchronization scheme, intended particularly for the narrowband LMR utilizing the studied digital modulation techniques. The evaluation criterion in form of power efficiency has been selected. In the first part, the radio channel convolving with the incoming signal is assumed to have fixed and constant frequency characteristics and be corrupted only by the presence of the AWGN having pre-defined parameters. In the second part, the robustness of the proposed system against the multipath fading process of selected parameters is simulated and evaluated. The particular parameters that have been used in the simulation can be found in [4], [19].

4.4.1 AWGN channel

The results of the complete communication system utilizing proposed synchronization scheme are presented in Figure 4.2.

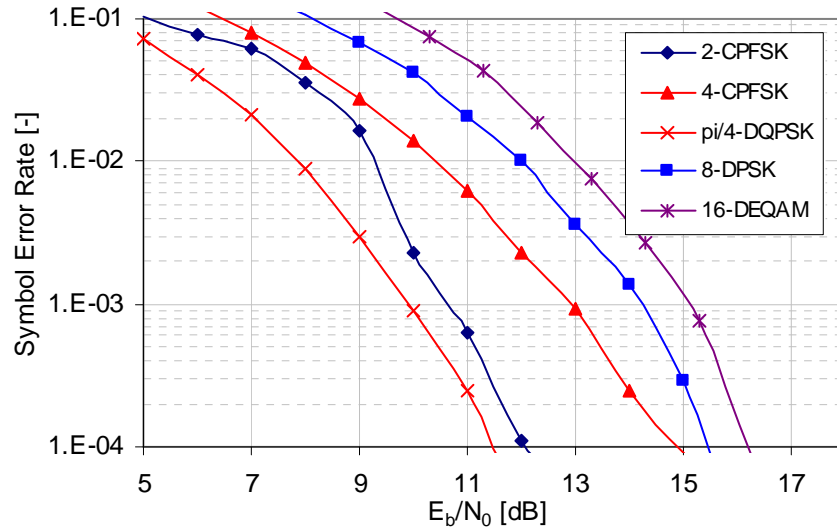


Figure 4.2: Power efficiency comparison for the selected modulation techniques. The complete synchronization mechanism (SWPC $L_0=16$, DDTED $\mu=0.1$) has been used; frame length 64 B.

It can be seen, that there is an influence of the initial correlation synchronization precision upon the overall symbol-error-rate of the system within the selected interval. The worsening is more evident for the low constellation ordering modulation 2-CPFSK in particular, while it requires the lowest *signal-to-noise* (SNR) to reach given *symbol-error-rate* (SER). In this interval,

the variance of the initial synchronization information, as provided by the sample wise pattern correlation, is dominant. The tracking part of the synchronization algorithm corrects the symbol timing precision during the time of the receiving frame as can be seen in Figure 4.3. However, it takes several symbol intervals that have higher likelihood of the incorrect symbol detection. In Figure 4.3 there are results of the synchronization performance analysis of the proposed synchronization scheme running in two modes. In the first mode, the synchronization task has been achieved using the sample wise pattern correlation technique, as derived in Section 4.2, while the tracking part of the algorithm has been disabled. In Figure 4.3 there are respective power efficiency characteristics of this mode assigned as “SWPC, $L_0=16$ ”. The second mode represents the complete synchronization scheme utilizing the acquisition and tracking mechanisms as they were formulated in previous chapters. The results are assigned as “SWPC, $L_0=16$, DDTED $\mu=0.1$ ”.

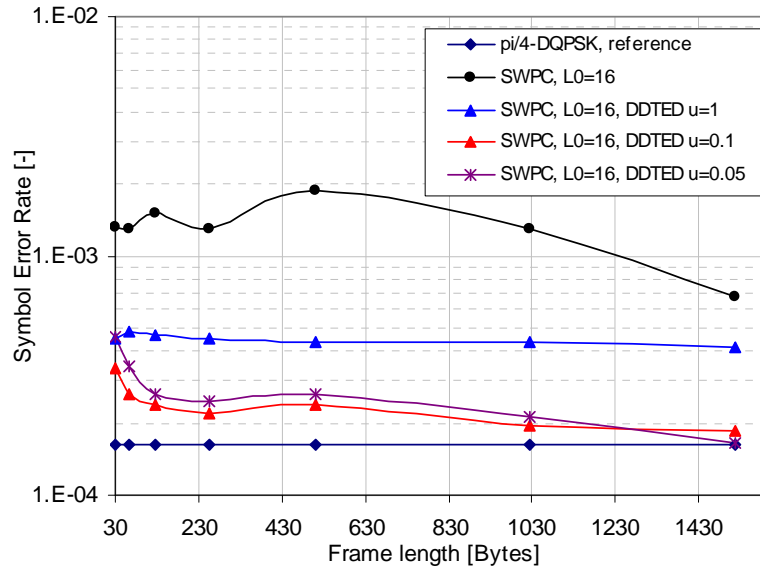


Figure 4.3: Results of the symbol error rate analysis of the synchronization algorithm for selected value of $E_b/N_0=11$ dB and different lengths of the test frames. $\pi/4$ -DQPSK.

Fastening the symbol timing recovery loop can improve the transient response, however, at a particular SNRs the inherent variance of the timing estimation would again cause an increase in probability of wrong symbol detection. Thus, to find the optimum value of the step-size parameter for the particular mode of operation it would require running a demanding optimization techniques (Figure 4.3). Nevertheless, even with selected value of the step-size parameter that has been set from the transient analysis described in [4], the performance penalty compared to optimally synchronized system power efficiency in an analyzed interval of symbol-error probabilities reaches 1 dB. This result can be judged acceptable for practical realization and the performance can be taken as a benchmark for the future synchronization algorithm improvements.

4.4.2 Rayleigh fading channel

There are two types of results presented for each fading process. Similarly to the previous section, the first set of results, shown in Figure 5.47 and Figure 5.48, depicts the dependency of the SER for the three modes of the symbol and frame timing synchronization of the narrowband digital receiver for selected modulation techniques and fixed frame length. In each plot, there is a reference characteristic for static “Static” and fading channel “REF” representing the respective modes of operation while the receiver is optimally synchronized. Two more characteristics assigned as “SWPC” and “DDTED” represent the results achieved by the digital receiver while it was synchronized by the proposed synchronization technique and it is either sample wise pattern

correlation technique alone “SWPC” or in combination with the decision directed timing recovery algorithm “DDTED”.

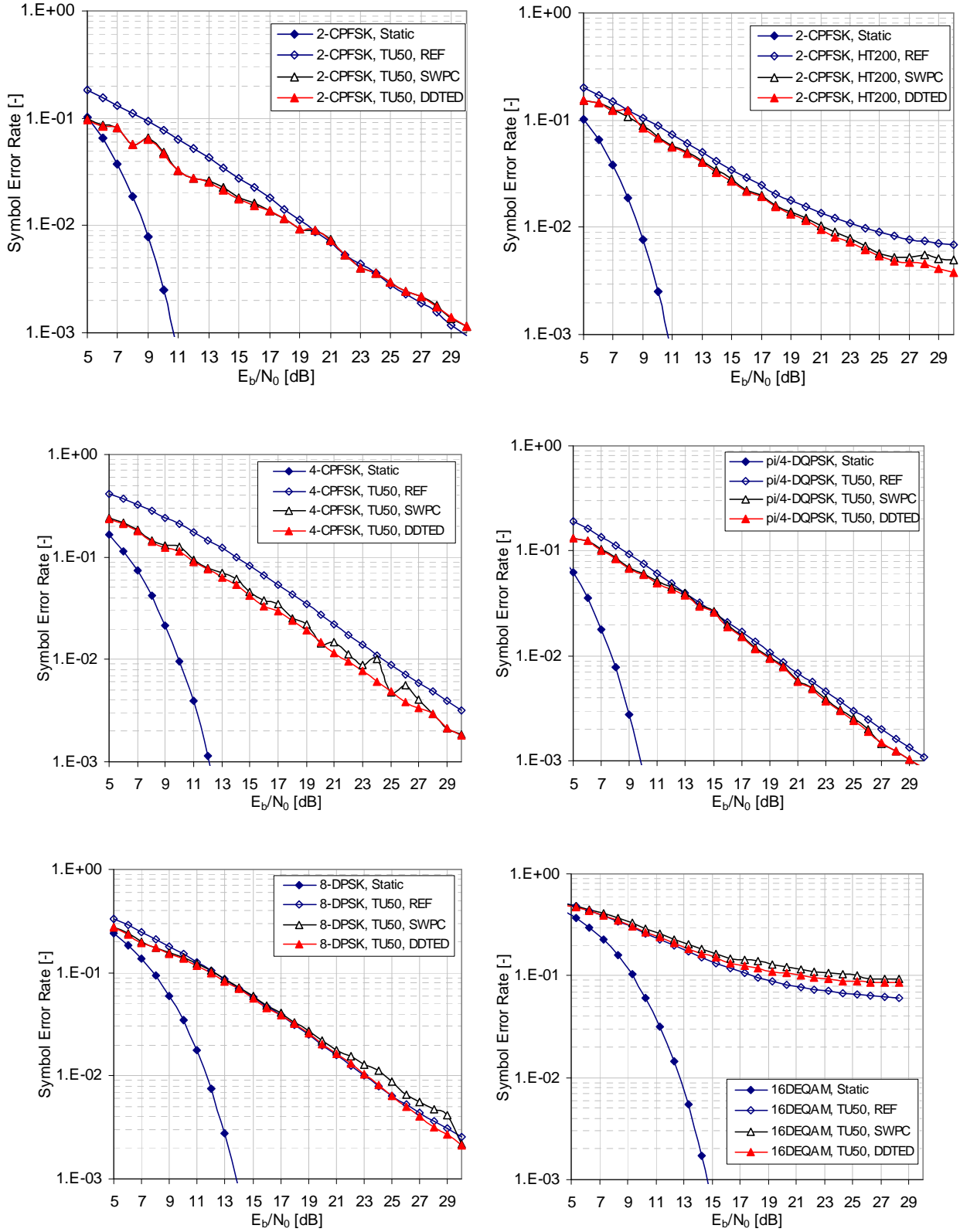


Figure 4.4: Results of the symbol error rate analysis for the three modes of the symbol and frame timing synchronization of the narrowband digital receiver under fading condition. SWPC $L_0=16$, DDTED $\mu=0.1$, frame length 64 B,

It can be seen from the results presented in Figure 4.4 that although the fading process significantly degrades the symbol-error behavior of narrowband receiver, the degradation is caused mostly by the reduction of the signal-noise-ratio while it is evident also in ideally synchronized receiver. The proposed synchronization mechanisms do not contribute to this degradation by any noteworthy portion. It is interesting to note that the adaptively synchronized system reaches in some particular modes of operation even lower values of SER. This phenomenon is most likely caused by the ability of the algorithm to trace the time variant optimum synchronization point. On the other hand, the possibility that the results are influenced by the particular property of the fading process cannot be completely foreclosed, although a significant effort has been spend to mitigate such influences by the long simulation runs and randomization of all simulation parameters including frame bytes, noise and fading processes for each level of E_b/N_0 . From the results presented, it is also clearly evident that without redundant information in form of forward-error-correction coding, the digital receiver is not able to reach sufficiently low values of symbol-error-rates. This fact becomes a significant problem with increasing spectral efficiency of the modulation techniques in D8PSK and 16-DEQAM.

5 PROTOTYPE RADIO MODEM ARCHITECTURES

Although the *software defined radio* (SDR) basic principles and various algorithms evaluations have been favored by a great interest in technical literature in recent years, there are only few references discussing the overall system performance when the SDR concept is employed in a narrowband radio transceiver design. The exceptions can be seen in references [21], [22], however, the specific aspects which take place in the design of narrowband communication system according to [1] differ and are not discussed. Moreover to the best of author's knowledge until the year of 2007, there had been no IF sampling digital narrowband radio modem fulfilling the ETSI EN 300 113 available on the market, and no narrowband radio modem utilizing any of the linear modulation schemes. Form this point view the work that begun in 2005 [6], [19], [23] can be considered fundamental and creates a significant part of the thesis contribution. There are two possible architectures of the narrowband IF sampling digital receiver analyzed in [4]. The main attention is given to achieve an understanding of the main limitation and compromises influencing the dynamic range performance of IF sampling digital receiver with a main emphasis on its practical implementation. In this section, only the most important simulation and measurement results of the IF over-sampling architecture are provided.

5.1 IF OVER-SAMPLING DIGITAL RECEIVER

The results of the essential radio parameters simulations are provided in Table 6.1. There are also the signal-to-noise ratios in respective locations of the simulation. The $SNR_{ADC} @ SER=10^{-2}$ represents the input signal-to-noise ratio with respect to the whole Nyquist zone for selected level of symbol-error-rate.

The $SNR_{ADC} @ -3dB Deg.$ represents the signal-to-noise ratio of the wanted signal and the simulated ADC noise signal that has been set for the degradation measurement without a presence of the interfering signal and without the inclusion of processing gain. And, the processing gain influenced SNR ratio is finally the one seen by the digital demodulator within the processed signal bandwidth.

From the simulation results, it can be seen that the strictest limits required for the co-channel rejection (-8 dB) can be fulfilled fully only in the 2-CPFSK mode of operation. For the spectrally more efficient techniques particularly the 4-CPFSK and $\pi/4$ -DQPSK this limit cannot be maintained without an additional forward-error-correction technique, however, it is reasonable to assume that with an acceptable amount of redundant information even the most enhanced forward error correction techniques prove to be short in delivering additional 4 to 5 dB in power efficiency. For even higher spectrally efficient modulation techniques the limit is far too severe to be fulfilled.

Table 5.1: Simulation results of the narrowband digital radio parameters in selected mode of operation.

Measurement bandwidth:			Nyquist zone			Occupied Bandwidth		Nyquist zone		
Modulation Format	Symbol Rate	Mod. Parameter	ADC Noise Level	SNR _{ADC} , @ SER 10 ⁻²	SNR _{ADC} , @ -3dB Deg.	SNR	Co-channel Rejection	Adjacent channel Selectivity	Blocking Ratio	IDR
[·]	[kBaud]	[·]	[dB]	[dB]	[dB]	[dB]	[dB]	[dB]	[dB]	[dB]
2CPFSK	13.08	$h=0.5, \alpha=0.28$	18.0	-2.0	1.0	6.8	-7.0	71.0	71.0	71.0
4CPFSK	12.00	$h=0.25, \alpha=0.28$	18.0	4.0	7.0	12.8	-13.0	65.0	65.0	65.0
$\pi/4$ -DQPSK	17.30	$\alpha=0.45$	18.0	3.0	6.0	11.5	-12.0	65.0	65.0	65.0
8DPSK	17.30	$\alpha=0.45$	18.0	6.0	9.0	16.0	-17.0	62.0	62.0	62.0
16-DEQAM	17.30	$\alpha=0.45$	18.0	11.0	14.0	19.5	-21.0	58.0	58.0	58.0

Two other parameters, in form of the adjacent channel selectivity, and radio blocking, determines the instantaneous dynamic range of the digital receiver [4]. It can be seen from Table 5.1, that the more spectrally efficient modulation technique, the higher value of the *SNR* is required. And while the instantaneous dynamic range requirements are constant it drives the need for widening the efficient dynamic range of the whole digital receiver. Thus, it can be concluded that the over-sampling digital narrowband receiver utilizing higher spectrally efficient modulation techniques fails to provide 70 dB of the adjacent channel selectivity and 84 dB of radio blocking in close vicinity of the nominal working frequency. However, compared to the sub-sampling architecture [4] the digital radio architecture utilizing the narrowband IF over-sampling subsystem can reach 14 dB wider effective dynamic range for the system parameters chosen. This value directly contributes to the 14 dB increase in instantaneous dynamic range of the digital receiver. Nonetheless, the selective analog front-end part is still inevitable to increase the selectivity of the software defined narrowband radio receiver if the higher spectrum efficiency of the data transmission is required.

5.2 MEASUREEEMENT RESULTS

The IF over-sampling receiver architecture has been designed for the narrowband LMR device. The software defined digital core containing both modems for exponential and linear modulations were implemented in *Altera Cyclone III EP3C10F256I8 FPGA* device [24]. The essential radio parameters of the complete radio transceiver were measured and the results are presented in this section.

In Figure 5.1, there are power efficiency characteristics measured for 2-CPFSK, 4-CPFSK and $\pi/4$ -DQPSK modes of operation. It can be seen that the *emf* sensitivity limit of +3 dB μ V is fulfilled for all modes when running at the symbol rate of 10.4 kBaud. When higher symbol rates are selected, the 4-CPFSK losses its power efficiency significantly and for the symbol rate of 13.08 kBaud it lowers down to the very edge of the admissible data sensitivity levels. Further increase of the exponential modulation spectrum efficiency can be therefore considered impractical. On the other hand, when using the $\pi/4$ -DQPSK, the radio receiver can still reach the data selectivity limit for 17.3 kBaud with a 2 dB margin.

The power efficiency characteristics for lower symbol rates were added to the plot as well in order to compare the properties of the modulation formats at the same spectrum efficiencies. As can be seen, at the symbol rate of 10.4 kBaud, both modulation formats reach almost the same data sensitivity (-113dBm @ BER 10⁻²). This is caused mainly due to the fact that there is higher frequency deviation used for 4-CPFSK at the lower symbol rates, thus the increase in power efficiency is not linear as for the $\pi/4$ -DQPSK. Even from this comparison it is evident that the $\pi/4$ -DQPSK mode of operation outperforms the 4-CPFSK at higher spectrum efficiencies.

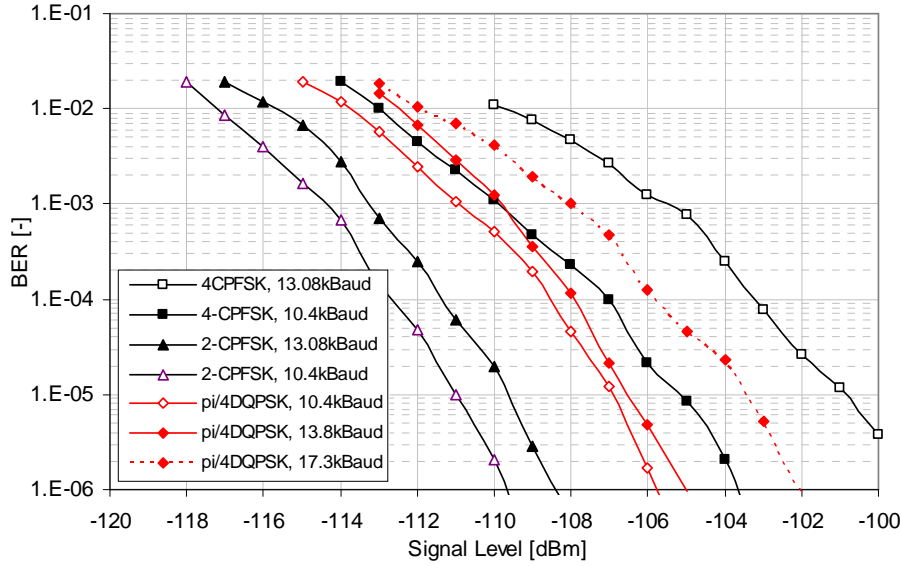


Figure 5.1: Results of the maximum usable sensitivity measurement of the narrow band receiver for 25 kHz channel bandwidth.

The second set of measurement results, collectively given in Table 5.2, describes the essential radio receiver parameters of the proposed IF over-sampling architecture. It is important to note that the measurement results are encumbered with a measurement uncertainty of ± 2 dB which is caused by *BER* estimation [4] as well as the inaccuracy of the measurement procedure itself. It already includes tolerances of the measurement equipments. The measuring procedures as well as the list of measurement instruments can be found in [4].

Table 5.2: Measurement results of the narrowband digital radio parameters in selected mode of operation at nominal frequency of 439.1 MHz.

Modulation Format	Symbol Rate	Mod. Parameter	Data Sensitivity @ BER 10^{-2}	Co-channel Rejection	Adjacent channel Selectivity	Blocking Ratio @ 1MHz offset
[-]	[kBaud]	[-]	[dBm]	[dB]	[dB]	[dB]
2-CPFSK	10.42	$h=0.75$, $\alpha=0.28$	-117	-7	77	96
	13.08	$h=0.5$, $\alpha=0.28$	-116	-8	75	96
4-CPFSK	10.42	$h=0.25$, $\alpha=0.28$	-113	-12	72	92
	13.08	$h=0.22$, $\alpha=0.28$	-110	-14	67	87
$\pi/4$ -DQPSK	10.42	$\alpha=0.45$	-114	-11	75	92
	13.08	$\alpha=0.45$	-113	-11	74	92
	17.30	$\alpha=0.45$	-112	-12	72	90
Measurement uncertainty ± 2 dB						

In accordance with the simulated results, only the 2-CPFSK mode of receiver operation fulfils the strict limit for the co-channel interference rejection. As it was concluded already in previous section, this limit – as required by [1] – is too severe and hinders the practical usage of spectrally more efficient modulation schemes while fulfilling limits of all essential radio parameters.

The decrease in power efficiency of the 4-CPFSK modulation at 13.08 kBaud causes the degradation of adjacent channel selectivity and while also the value of data sensitivity is near the requested limit, this mode can be judged the least suitable for the efficient narrowband channel usage.

5.3 EFFICIENT USE OF THE RADIO CHANNEL

The measurement results presented in the previous section can be used to analyze the communication efficiency of narrowband radio channel utilization by direct comparison to the Shannon bound [5], [4]. The graphical comparison is provided in Figure 5.2.

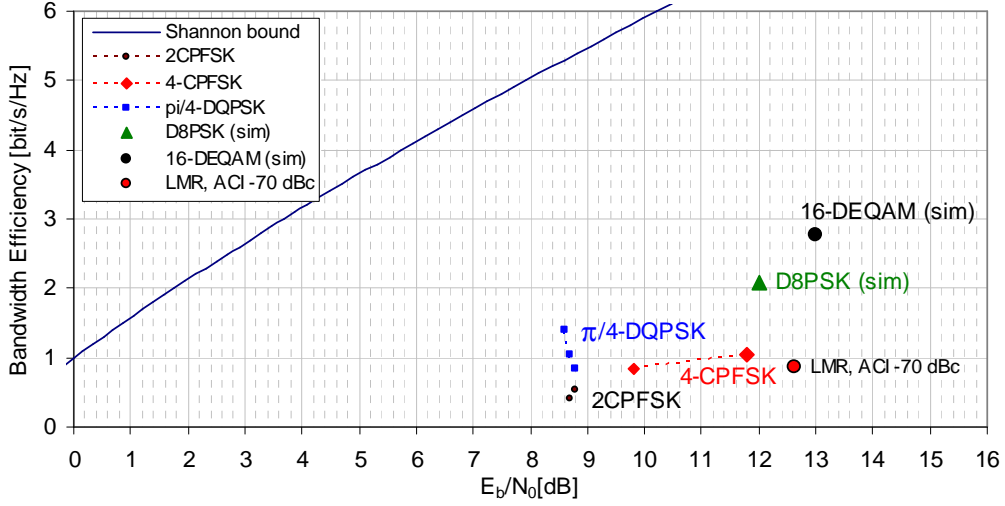


Figure 5.2: Graphical comparison of the spectrum and power efficiency for the applicable modes of the narrowband LMR operation (Table 5.2). $NF=8$ dB, $B_N=25$ kHz, $BER=10^{-2}$.

Although the results presented are based on measurement values, and thus, they are encumbered with systematic errors – either in *noise figure* (NF) estimation, BER calculation, measurement uncertainty, various algorithms imperfection etc. – the ambition is to compare the communication efficiency as close to the real application of the narrowband LMR as possible.

It can be seen in Figure 5.2 that for the 4-CPFSK modulation the distance from the Shannon bound is increasing significantly with only moderate increase in spectrum efficiency. This is not the case for $\pi/4$ -DQPSK. With increasing the spectrum efficiency within the fixed bandwidth, the required value of E_b/N_0 remains almost constant and thus, the communication efficiency approaches towards optimal communication system. Therefore, it can be concluded that the LMR systems utilizing proposed mode of operation uses the assigned bandwidth more effectively. Compared to the up-to-date LMR systems – $R_b=21.68$ kb/s, $B_N=25$ kHz, $S=-110$ dBm ($BER=10^{-2}$), $NF=8$ dB is assumed – that were subject to ACI limit of -70 dBc, the distance is even more evident. At the current state of the project, the D8PSK and 16-DEQAM modes have not yet been implemented, however when the simulated values of the spectrum and power efficiencies are compared in Figure 5.2, it can be seen that the communication efficiency is not increased, even though the spectrum efficiency is higher.

Based on the above comparison it can be also concluded that the main ambition of the dissertation thesis presented *...to find a practical way how to combine efficient signaling techniques together with the modern digital methods for fast frame and symbol synchronization in order to increase the efficiency of the narrowband radio channel usage allocated to the new generation of the industrial narrowband LMR system...* has been reached successfully. The particular contributions of this dissertation project and practical recommendations towards meeting this objective are summarized in the final chapter.

6 CONCLUSION AND FUTURE WORK

Digital modulations for narrowband radio channel

As shown in [4] and measurement results presented in Section 5, the higher level of admissible adjacent channel interference in addition to the proposed pulse shaping technique enable 10% raise in spectrum efficiency of the exponential digital modulation, from the value of 0.87 bit/s/Hz (21.68 kbit/s @ 25 kHz) to 0.96 bit/s/Hz (24 kbit/s @ 25kHz). However, when overall power efficiency is of the primary application concern, the additional increase in frequency deviation can be recommended instead of increasing the modulation rate. Thus, the 2-CPFSK modulation having $h=0.75$ and resulting spectrum efficiency approaching 0.5 bit/s/Hz can be a suggested option.

When higher symbol rates are selected the 4-CPFSK losses its power efficiency significantly and therefore the distance from optimal system is increasing rapidly (Figure 5.2). Moreover, for the symbol rate of 13.08 kBaud it lowers down to the very edge of the admissible data sensitivity limit -110 dBm. Further increase of the exponential modulation spectrum efficiency from the values currently being used can be therefore considered inefficient.

From all the modulation formats studied, the $\pi/4$ -DQPSK can provide the narrowband LMR system with communication efficiency closest to the optimal communication systems. The proposed solution based on this modulation format can reach the spectrum efficiency of 1.5 bit/s/Hz. The data sensitivity limit required by [1] can also be fulfilled with a margin of 2-3 dB.

Additional increase in spectrum efficiency can be gained by D8PSK and 16-DEQAM modulation formats. However, compared to $\pi/4$ -DQPSK, an increase in overall communication efficiency cannot be expected, while there is a penalty in power efficiency characteristic. Without significant amount of redundant information in form of forward-error-correction coding, also the current (absolute) limit of data sensitivity -110 dBm, which does not take into account the spectrum efficiency of the mode of operation considered, cannot be met.

As it was shown by the system simulations presented in Chapter 4.4.2, the robustness against multipath fading effects is becoming a critical issue when higher order modulation techniques are considered. Therefore, prior to the practical implementation of the spectrally more efficient modes of operation, an effective algorithm for narrowband radio channel equalization would be required. The multicarrier modulation technique such as *filtered bank multi-carrier modulation* (FBMCM) [8] in combination with adaptive channel equalizer can be an option. It is assumed that in this case, the current network topology as well as the channel access techniques should be a subject of the further analysis.

Pulse shape filtering

The Nyquist δ -filters derived in Chapter 3.3 provide the narrowband digital modem with higher adjacent channel attenuations required with only a half of the filter impulse response group delay compared to truncated raised cosine filters. The group delay parameter determines the digital filter order and more importantly, it is the main contributor to the signal propagation delay in a digital signal processing part of the modem. The resultant occupied bandwidth of the linearly modulated signal makes the usage of high symbol rates of up to 18 kBaud applicable while the shape of the main lobe positively affects the PAPR which remains very close to the optimum values simulated [4]. An exact symbolic definition of the Nyquist δ -filter in the frequency domain gives the designer scope to choose freely the filter parameters such as equivalent excess bandwidth, group delay and over-sampling parameters and derive coefficients for either the “normal” or the square root filter variants.

Nyquist (M) filters as derived in [25] can also be recommended for practical implementation while the optimization design technique enables additional trade-off between inter-symbol interference and out-of-band interference suppression.

Digital algorithms for frequency discrimination

The algorithms for frequency discrimination represent a typical class of the non-linear signal processing tasks and with an exception of the digital phase locked loop with its combined feed-forward and feedback architecture they use approximation techniques and are limited by a nature of the signal sampling in time. In particular, the approximation of the derivation process by a discrete time differentiation yields to higher over sampling rates in order to reduce the approximation imperfection [4].

Two main modifications to the more general formulations of the frequency discriminators have been proposed in [4]. The modifications improve the demodulators' behavior at low SNR levels that are important for the maximum usable data sensitivity of the narrowband LMR and in marginal operating conditions (e.g. the radio modem being blocked by a strong interferer).

From all the studied algorithms the *normalized digital phase locked loop* (DPLL) utilizing the proposed *averaging filter* reaches the best results. However, it has the most demanding realization structure combining feedback and feed-forward architecture. The *modified mathematic demodulator* can be classified a preferable frequency discrimination algorithm for the narrowband LMR radio modems, since it can be effectively realized by a feed-forward architecture and has the SNR penalty of 0.5 dB compared to the normalized DPLL algorithm with the averaging filter.

Rapid frame and symbol synchronization

In order to implement efficient frame and symbol synchronization algorithm in narrowband LMR system, the following recommendations can be derived based on Chapter 4.

Sample wise pattern correlator in its simplified and effective form (4.5) and (4.11) for the exponential and linear modulation techniques respectively can be used as the frame synchronization algorithm as well as for the initial timing estimation. Further analysis of the autocorrelation properties of the various pseudo-noise and random sequences can result in even better synchronization performance than the one presented. However, based on the simulated and measured results it can be concluded that the algorithm is proved to provide efficient symbol synchronization method in future narrowband LMR systems.

Decision directed timing estimate detector in its unified realization structure based on (4.18) and (4.22) can be used to correct the sampling instant over the entire receiving frame. The proposed version of the algorithm does not require any redundant information and forms a low complexity, all-digital solution.

Fractional interpolator with linear or parabolic interpolation polynomial analyzed in [4], [17] can be used as the main timing adjustment algorithm. For the over-sampling factor exceeding 5 signal samples per modulation symbol, even the simplest interpolator with linear interpolation polynomial can be used without noteworthy system degradation.

The results of the overall system simulations (Section 4) demonstrate that the proposed synchronization algorithm recovers frame and symbol synchronization with practically acceptable penalty in power efficiency – comparing to the optimally synchronized radio receiver – reaching 1 dB in an analyzed interval of the symbol-error-rates. The overall algorithm requires 16 known symbols to acquire the initial timing estimate. The algorithm can be used for all digital modulation formats studied and excess bandwidths down to 20%. The performance characteristics of the proposed synchronization algorithm can be taken as a benchmark for future synchronization algorithm enhancements.

Narrowband radio system architecture

Following practical recommendation can be derived based on the experimental part of this dissertation project [4].

For the practical design of the narrowband radio receiver with an IF sampling digital part, the appropriate combination of the selective analog front-end together with the high performance digital receiver is still inevitable in order to improve the data sensitivity, adjacent channel selectivity and to extend the instantaneous dynamic range of the whole narrowband receiver.

There were two possible *IF sub-sampling* and *IF over-sampling* architectures analyzed in this project in order to fulfil the design objective of narrowband radio receiver.

By comparing the measurement results describing the instantaneous dynamic range of the sub-sampling and over-sampling architecture it can be concluded, that the IF over-sampling architecture reaches substantially wider dynamic range. The main reason can be seen in the efficient proprietary implementation of the higher sampling frequencies that are needed to widen the instantaneous dynamic range of the digital part.

There is a possibility to use the sub-sampling technique in modern IF-sampling narrowband receivers, in order to lower the required sampling frequency. However, the sampling frequency cannot be lowered arbitrarily. It is necessary to use significantly higher sampling frequencies, compared to the occupied signal bandwidth, to widen the overall instantaneous dynamic range of the narrowband receiver. While increasing the sampling frequency significantly increases price and consumed power of the digital part, the architectures based on IF sub-sampling technique can be classified impractical for the high performance narrow band radio receiver.

Although the digital filters bear a major part of the channel selectivity, the proposed architectures of the IF sampling digital receiver do not reach the required values of instantaneous dynamic range in close and farther distance from the nominal carrier frequency. The use of anti-aliasing filters with steep band-pass response is still inevitable for the intended analog front-end system. This part can be seen as the main restrictive element in the narrowband radio receiver architecture that dominantly limits the flexibility of the whole equipment, especially when it comes to processed bandwidths applicable. This limitation is considered a main disadvantage of both architectures proposed.

Technical parameters of the narrowband receiver

Maximum Usable Data sensitivity (-110 dBm): limit can be fulfilled by the proposed narrowband radio receiver for spectrum efficiencies reaching 1.5 bit/s/Hz using $\pi/4$ -DQPSK, and lower for 2-CPFSK and 4-CPFSK modulation formats. For additional increase in spectrum efficiency the absolute limit of data sensitivity imposes an impractical constraint. It is therefore reasonable to advise the modification of the present standard [1], in order to make use of higher spectrally efficient modulation techniques by the LMR system operating in LBT mode possible. In this way, the spectrum efficiency of the narrowband systems can be increased.

Co-channel interference rejection (0 dB to -8 dB): without additional forward-error-correction techniques this limit can be fulfilled only in 2-CPFSK mode of operation. As it was concluded in Section 5, this limit is too severe and hinders the practical usage of spectrally more efficient modulation schemes while meeting limits of all essential radio parameters. Adequate lowering of the limit being subject to increased spectrum efficiency should be advised, without the risk of assigned spectrum misuse. As it was shown in Chapter 5.3, contrary can be expected the case, especially in $\pi/4$ -DQPSK mode of operation.

Adjacent channel selectivity (70 dB): while this limit is met for 2-CPFSK mode of operation, it is becoming difficult to reach this limit with higher spectrally efficient modulation techniques 4-CPFSK, $\pi/4$ -DQPSK. The limitation is caused mainly by two factors. Firstly, it is the limited instantaneous dynamic range of the IF sampling digital radio part which can be improved using strictly selective analog front-end part while abnegating the flexibility of the overall radio

construction. Secondly, it is the absolute level of the phase noise of first receiver local oscillator which cannot – or it is highly impractical to – be lowered to the limits that would be required for high spectrally efficient techniques such as D8PSK and 16-DEQAM. Natural lowering of this limit with increasing spectrum efficiency of the mode of operation is therefore advisable. The absolute power level (e.g. -37 dBm) of the interfering signal that the radio receiver has to withstand while operating near (+3 dB) the specified data sensitivity limit would be the suggested modification to the present standard, without the risk of future communication system co-existence problems.

Blocking and desensitization (84 dB): the same holds true for the radio blocking and desensitization of the radio receiver in close vicinity (below 1 MHz) to the nominal carrier frequency. While typically, it is not critical to fulfill limit of this parameter at the frequency offsets exceeding 1 MHz, below this value, the residual level of the first receiver local oscillator phase noise is becoming a limiting factor. In any case, again the absolute power level (e.g. -23 dBm) of the interfering signal that the radio receiver has to withstand while operating near (+3 dB) the specified data sensitivity limit would be the suggested modification to the present standard, without the risk of future communication system co-existence problems.

REFERENCES

- [1] ETSI EN 300 113-1 V1.6.2 (2009-11), Electromagnetic compatibility and Radio spectrum Matters (ERM), Part 1: Technical characteristics and methods of measurement. *European Standard*. ETSI, 11/2009.
- [2] JESUALE, N., EYDT, C. B. A Policy Proposal to Enable Cognitive Radio for Public Safety and Industry in the Land Mobile Radio Bands. In *2nd IEEE International Symposium on New Frontiers in Dynamic Spectrum Access Networks. DySPAN 2007*. 10.1109/DYSPAN.2007.16.
- [3] DANĚK, K. *Efektivní využití rádiového kanálu pro přenos dat*, Dissertation Thesis, VUT Brno, 2001.
- [4] BOBULA, M. *Contribution to efficient use of the radio channel*. Brno: Brno University of technology, Faculty of Electrical Engineering and Communication, 2011. 170 s. Thesis Supervisor doc. Ing. Aleš Prokeš, Ph.D.
- [5] BURR, A. *Modulation and Coding for Wireless Communications*. Harlow: Pearson Education Ltd. 2001. 360 pages. ISBN 0 201 39857 5.
- [6] BOBULA, M. *Use of Radio Channel 200 kHz for data transmission*. MSc. Diploma Thesis, University of Technology BRNO, 2006.
- [7] SKLAR, B., Rayleigh Fading Channels in Mobile Digital Communication Systems Part I: Characterization. In *IEEE Communication Magazine 1997*. IEEE, July, 1997.
- [8] ETSI TS 100 392-2 V3.1.1, “Terrestrial trunked radio (TETRA); Voice plus Data (V+D); Part 2: Air Interface (AI). *Technical specification*, ETSI 10/2008.
- [9] MORELLI M., MENGALI U. Joint frequency and timing recovery for MSK-type modulation. In *IEEE Trans. on Commun.*, Vol.47, No. 6, June 1999, p. 938 – 946.
- [10] SVENSSON, N., A., B. On Differentially Encoded Star 16QAM with Differential Detection and Diversity. In *IEEE Transaction on Vehicular Tech.* Vol. 44, No. 3, August 1995.
- [11] FONSEKA, J., Baseband pulse shaping to reduce intersymbol interference in Narrowband M-ary CPFSK Signaling. In *Tenth Annual International Phoenix Conference on Computers and Communication*, 1991, CH2859-5/91/0000/0393.

- [12] FX919, 4-level FSK modem data pump, *CML Semiconductor product datasheet*, July 1997.
- [13] BOBULA, M., PROKEŠ, A., DANĚK, K. Nyquist Filters with Alternative Balance between Time- and Frequency-domain Parameters. In *EURASIP Journal on Advances in Signal Processing*. Volume 2010, Accepted for publication 2010-10-28.
- [14] HARRIS, J. F. On the use of windows for harmonic analysis with the discrete Fourier transform. In *Proceedings of the IEEE*. Vol. 66, No. 1, January 1978.
- [15] BEAULIEU, C. N., et al., A “Better Than” Nyquist Pulse. In *IEEE Communications Letters*. Vol. 5, No.9, September 2001., p. 367-368.
- [16] JAN, J. *Digital Signal Filtering, Analysis and Restoration*.(in Czech) VUTIUM BUT, BRNO. 2002. ISBN 80-214-2911-9.
- [17] BOBULA, M., Design of the fractional delay interpolators based on Farrow structure. (in Czech), [Online] Cited 2010-06-13. Available at: <http://www.elektrorevue.cz/cz/clanky/zpracovani-signalu/5/navrh-cislicovych-filtru-se-spojite-promennou-hodnotou-zpozdeni-na-bazi-farrowova-interpolatoru/>
- [18] BOBULA, M., DANĚK, K., PROKEŠ, A., Simplified frame and symbol synchronization for 4-CPFSK with $h=0.25$. In *Radioengineering*, vol.17, no. 2, June 2008, ISSN 1210-2512. [Online] Cited 2010-10-03. Available at: http://www.radioeng.cz/fulltexts/2008/08_02_108_114.pdf
- [19] BOBULA, M., DANĚK, K., PROKEŠ, A. Implementation of Industrial Narrow Band Communication System into SDR concept. In *Radioengineering*, vol. 17, no. 4, December 2008. [Online] Cited 2010-10-02. Available at: http://www.radioeng.cz/fulltexts/2008/08_04a_086_092.pdf
- [20] DANĚK, K. Efficient use of mobile radio channel II. In *Radioengineering*, June 2000, vol. 9, no.2, p.1-4. [Online] Cited 2010-10-02. Available at: http://www.radioeng.cz/fulltexts/2000/00_02_01_04.pdf
- [21] DODLEY, J., P., ERVING, R., H., RICE, C.W., In-building software radio architecture, design and analysis., In *The tenth IEEE International Symposium on Personal, Indoor and Mobile Radio Communications*, PIMRC 2000, 10.1109/PIMRC.2000.881470.
- [22] LAWTON, M., C., Sensitivity analysis of radio architectures employing sample and hold techniques. In *Radio rec. and assoc. syst. 1995*, Conf. publication No. 415, pp. 52-56.
- [23] BOBULA, M. FPGA Implementation of an SDDR Core for Radio Transceiver. In *STUDENT EEICT 2006*. vol. 2. VUT BRNO, 2006. p. 14 - 16, ISBN-80-214-3161-X.
- [24] ALTERA Corp., *Cyclone III Device Handbook*, CIII5V1-3.3. [online] 2010-10-31, Available at: http://www.altera.com/literature/hb/cyc3/cyc3_ciii5v1.pdf
- [25] FARHANG-BOROUJENY, B. A universal square-root Nyquist (M) filter design for digital communication systems. In *Proceeding of the SDR 06 Tech Conference*. SDR forum 2006.

CURRICULUM VITAE

Name, surname: **MAREK BOBULA**
Date of birth: 4th of May, 1983
Home address: Hájová 677/4, Svit, 059 21, Poprad region, Slovak Republic
Temporary address: K Čimperku 1838, Tišnov, 666 01, Brno-venkov region, Czech Republic
E-mail address: bobula.marek@gmail.com
Nationality: Slovak
Marital status: married

Education:

2006 – 2010 Brno University of Technology / Department of Radio Electronics
Doctoral study in Electronics and communication
2001 – 2006 Brno University of Technology / Department of Radio Electronics
MSc. study in Electronics and communication. Graduated with honor

Awards:

2006 Preciosa scholarship 2006
2006 MSc. Thesis Dean award

Student competitions:

04/2006 Student EEICT 2006, 1. place
Section: M4 – Electronics and communication
Contribution: FPGA implementation of an SDDR core for radio transceiver
05/2005 Honeywell EMI 2005, 2. place
Section: Electronics and Information technologies – MSc. projects
Contribution: Automatic measurement application for car-use TV tuner
04/2005 Student EEICT 2005, 1. place
Section: Electronics telecommunication and automatization
Contribution: Automatic measurement application for car-use TV tuner

Work experience:

2004–present RACOM Ltd., Czech Republic
HW and SW development in a field of digital signal processing
06-09/2006 Manipal Institute of Technology, India
International student internship at the Department of Electronics
06-09/2004 Alps Electric, Japan
International student internship in RF development centre

Other Skills:

Languages **English**, advanced; **German**, beginner; **Slovak**, native

ABSTRACT

The industrial narrowband *land mobile radio* (LMR) devices, as considered in this dissertation project, has been subject to *European standard ETSI EN 300 113*. The system operates on frequencies between 30 MHz and 1 GHz, with channel separations of up to 25 kHz, and is intended for *private, fixed, or mobile, radio packet switching networks*. Data telemetry, SCADA, maritime and police radio services; traffic monitoring; gas, water, and electricity producing factories are the typical system applications. *Long distance coverage, high power efficiency, and efficient channel access techniques in half duplex operation* are the primary advantages the system relays on. Very low level of *adjacent channel power emissions* and robust *radio receiver architectures*, with *high dynamic range*, enable for a system's coexistence with various communication standards, without the additional guard band frequency intervals.

On the other hand, the strict limitations of the referenced standard as well as the state of the technology, has hindered the increase in *communication efficiency*, with which the system has used its occupied bandwidth. New modifications and improvements are needed to the standard itself and to the up-to-date architectures of narrowband LMR devices, to make the utilization of more efficient modes of system operation practically realizable.

The main objective of this dissertation thesis is therefore to find a practical way how to combine the favorable properties of the advanced nonlinear and linear digital modulation techniques in a single digital modem solution, in order to increase the efficiency of the narrowband radio channel usage allocated to the new generation of the industrial LMR devices.

The main attention is given to the particular areas of digital modem design such as proposal of the *new family of the Nyquist filters minimizing the adjacent channel interference*, design and analysis of the *efficient algorithms for frequency discrimination, fast frame and symbol timing recovery* as well as to the *analysis of the software defined receiver performance* under *additive white Gaussian noise* (AWGN) and *multipath fading* radio channel conditions. There are also main results presented from the practical part of this dissertation project, while designing and analyzing two prototyping architectures of the narrowband software defined radio modems. In this part, in addition, the conditions and practical recommendations towards using spectrally efficient modulation techniques in future narrowband LMR devices are provided.

ABSTRAKT

Předkládaná práce se soustředí na problematiku využívání úzkopásmového rádiového kanálu *rádiovými modemy*, které jsou určené pro *průmyslové aplikace pozemní pohyblivé rádiové služby*, specifikované v dominantní míře *Evropským standardem ETSI EN 300 113*. Tato rádiová zařízení se používají v kmitočtových pásmech od 30 MHz do 1 GHz s nejčastěji přidělovanou šířkou pásma 25 kHz a ve většině svých instalací jsou využívána ve *fixních nebo mobilních bezdrátových sítích*. Mezi typické oblasti použití patří zejména datová telemetrie, aplikace typu SCADA, nebo monitorování transportu strategických surovin. Za hlavní znaky popisovaného systému lze označit komunikační pokrytí značných vzdáleností, dané především vysokou výkonovou účinností datového přenosu a využívání efektivních přístupových technik na rádiový kanál se semiduplexním komunikačním režimem. Striktní požadavky na elektromagnetickou kompatibilitu umožňují těmto zařízením využívat spektrum i v oblastech kmitočtově blízkým jiným komunikačním systémům bez nutnosti vkládání dodatečných ochranných frekvenčních pásem.

Úzkopásmové rádiové komunikační systémy, v současnosti používají převážně exponenciální digitální modulace s konstantní modulační obálkou zejména z důvodů velice striktních omezení pro velikost výkonu vyzařeného do sousedního kanálu. Dosahují tak pouze kompromisních hodnot *komunikační účinnosti*. Úpravy limitů příslušných rádiových parametrů a rychlý rozvoj prostředků číslicového zpracování signálu v nedávné době, dnes umožňují ekonomicky přijatelné využití spektrálně efektivnějších modulačních technik i v těch oblastech, kde je prioritní využívání úzkých rádiových kanálů.

Cílem předkládané disertační práce je proto výzkum postupů směřující ke sjednocení výhodných vlastností lineárních a nelineárních modulací v moderní konstrukci úzkopásmového rádiového modemu. Účelem tohoto výzkumu je efektivní a „ekologické“ využívání přidělené části frekvenčního spektra.

Mezi hlavní dílčí problémy, jimiž se předkládaná práce zabývá, lze zařadit zejména tyto: *Nyquistova modulační filtrace, navrhovaná s ohledem na minimalizaci nežádoucích elektromagnetických interferencí, efektivní číslicové algoritmy frekvenční demodulace a rychlé rámcové a symbolové synchronizace*. Součástí práce je dále analýza navrhovaného řešení z pohledu celkové konstrukce programově definovaného rádiového modemu v rovině simulací při vyšetřování robustnosti datového přenosu *rádiovým kanálem s bílým Gaussovským šumem* nebo *kanálem s únikem* v důsledku mnohacestného šíření signálu.

Závěr práce je pak zaměřen na prezentování výsledků praktické části projektu, v níž byly testovány, měřeny a analyzovány dvě prototypové konstrukce rádiového zařízení. Tato finální část práce obsahuje i praktická doporučení, vedoucí k vyššímu stupni využitelnosti spektrálně efektivnějších komunikačních režimů v oblasti budoucí generace úzkopásmových zařízení pozemní pohyblivé rádiové služby.